MOLECULAR AND CELLULAR BIOLOGY, June 2010, p. 2775–2786 Vol. 30, No. 11
0270-7306/10/$12.00 doi:10.1128/MCB.00151-10

Specificity and Stoichiometry of Subunit Interactions in the Human Telomerase Holoenzyme Assembled *In Vivo*▽

Emily D. Egan and Kathleen Collins*

Department of Molecular and Cell Biology, University of California at Berkeley, Berkeley, California 94720

Received 5 February 2010/Returned for modification 15 March 2010/Accepted 18 March 2010

The H/ACA motif of human telomerase RNA (hTR) directs specific pathways of endogenous telomerase holoenzyme assembly, function, and regulation. Similarities between hTR and other H/ACA RNAs have been established, but differences have not been explored even though unique features of hTR H/ACA RNP assembly give rise to telomerase deficiency in human disease. Here, we define hTR H/ACA RNA and RNP architecture using RNA accumulation, RNP affinity purification, and primer extension activity assays. First, we evaluate alternative folding models for the hTR H/ACA motif 5′ hairpin. Second, we demonstrate an unanticipated and surprisingly general asymmetry of 5′ and 3′ hairpin requirements for H/ACA RNA accumulation. Third, we establish that hTR assembles not one but two sets of all four of the H/ACA RNP core proteins, dyskerin, NOP10, NHP2, and GAR1. Fourth, we address a difference in predicted specificities of hTR association with the holoenzyme subunit WDR79/TCAB1. Together, these results complete the analysis of hTR elements required for active RNP biogenesis and define the interaction specificities and stoichiometries of all functionally essential human telomerase holoenzyme subunits. This study uncovers unexpected similarities but also differences between telomerase and other H/ACA RNPs that allow a unique specificity of telomerase biogenesis and regulation.

The challenge of eukaryotic chromosome end replication is met in part by telomerase-mediated synthesis of terminal DNA repeats (19). The telomerase catalytic core can be reconstituted from telomerase reverse transcriptase (TERT) and telomerase RNA (TER), which together form a specialized reverse transcriptase enzyme (35). Although the sequences and structures of TERs are highly divergent across eukaryotes, all TERs contain three elements important for RNP catalytic activity: an internal template for telomeric repeat synthesis, an adjacent pseudoknot, and a distantly positioned stem terminus element (3). TERs also contain motifs that mediate RNA folding, stability, localization, and regulation *in vivo* (9). In vertebrate cells, the TER precursor is transcribed by RNA polymerase (Pol) II. The 451-nucleotide (nt) mature human telomerase RNA (hTR) is produced by 3′ end trimming and 5′ end modification with a trimethylguanosine (TMG) cap (15, 17, 21, 28). Consistent with the requirement for a specific pathway of biogenesis, mature hTR accumulation is favored by Pol II expression contexts lacking a downstream signal for transcription-coupled mRNA or small nuclear RNA (snRNA) 3′ end formation (16).

The 5′ half of hTR resembles a compact ciliate TER, with the template and pseudoknot constrained by a domain-closing stem, while the 3′ half adopts a fold shared by a large family of H/ACA motif small nucleolar RNAs (snoRNAs) and small Cajal body RNAs (scaRNAs) (Fig. 1A). H/ACA snoRNAs and scaRNAs function predominantly as guides for the site-specific pseudouridylation of rRNA and snRNA, respectively (27). The canonical secondary structure of a eukaryotic H/ACA RNA consists of a 5′ hairpin followed by a single-stranded H box (ANANNA) and then a 3′ hairpin followed by a single-stranded ACA located 3 nt from the mature RNA 3′ end (20). Each hairpin contains an internal loop or "pocket" that guides the selection of a modification target. Both sides of an unpaired stem pocket base pair to the target RNA such that the target uridine is extruded from the hybrid at the top of the pocket (13, 25). Putative modification guide sequences of vertebrate TERs are not conserved, suggesting that TERs do not direct RNA modification. Also, while hTR is an independent transcript trimmed at its 3′ end, other vertebrate H/ACA RNAs are both 5′ and 3′ end processed from introns. Despite these differences, *in vivo* accumulation of hTR requires the same H box and ACA elements required for snoRNA accumulation (28, 29). By directing a specific pathway of primary transcript maturation and RNP biogenesis, the hTR H/ACA motif provides a mechanism for efficient assembly of a biologically stable telomerase RNP.

Canonical H/ACA RNAs share the RNP core proteins Cbf5/NAP57/dyskerin (the pseudouridine synthase), NOP10, NHP2, and GAR1 (32). The heterotrimer of dyskerin, NOP10, and NHP2 is deposited onto each hairpin unit of the H/ACA motif in a highly chaperoned biogenesis process (27). Cotranscriptional association of the heterotrimer is followed by an exchange of biogenesis factors for the fourth core subunit, GAR1, to produce a biologically functional RNP (11). All four H/ACA RNP proteins copurify hTR as well as other H/ACA RNAs. The three core heterotrimer proteins can be detected by mass spectrometry of purified human telomerase holoenzyme (18) although one report has suggested that holoenzyme includes only dyskerin, hTR, and TERT (7). Recent structures of reconstituted archaeal single-stem RNPs with Cbf5, Nop10, and the NHP2-related protein L7Ae indicate that Cbf5 con-

* Corresponding author. Mailing address: Department of Molecular and Cell Biology, 331 LSA, University of California, Berkeley, CA 94720-3200. Phone: (510) 643-1598. Fax: (510) 643-6791. E-mail: kcollins@berkeley.edu.

▽ Published ahead of print on 29 March 2010.

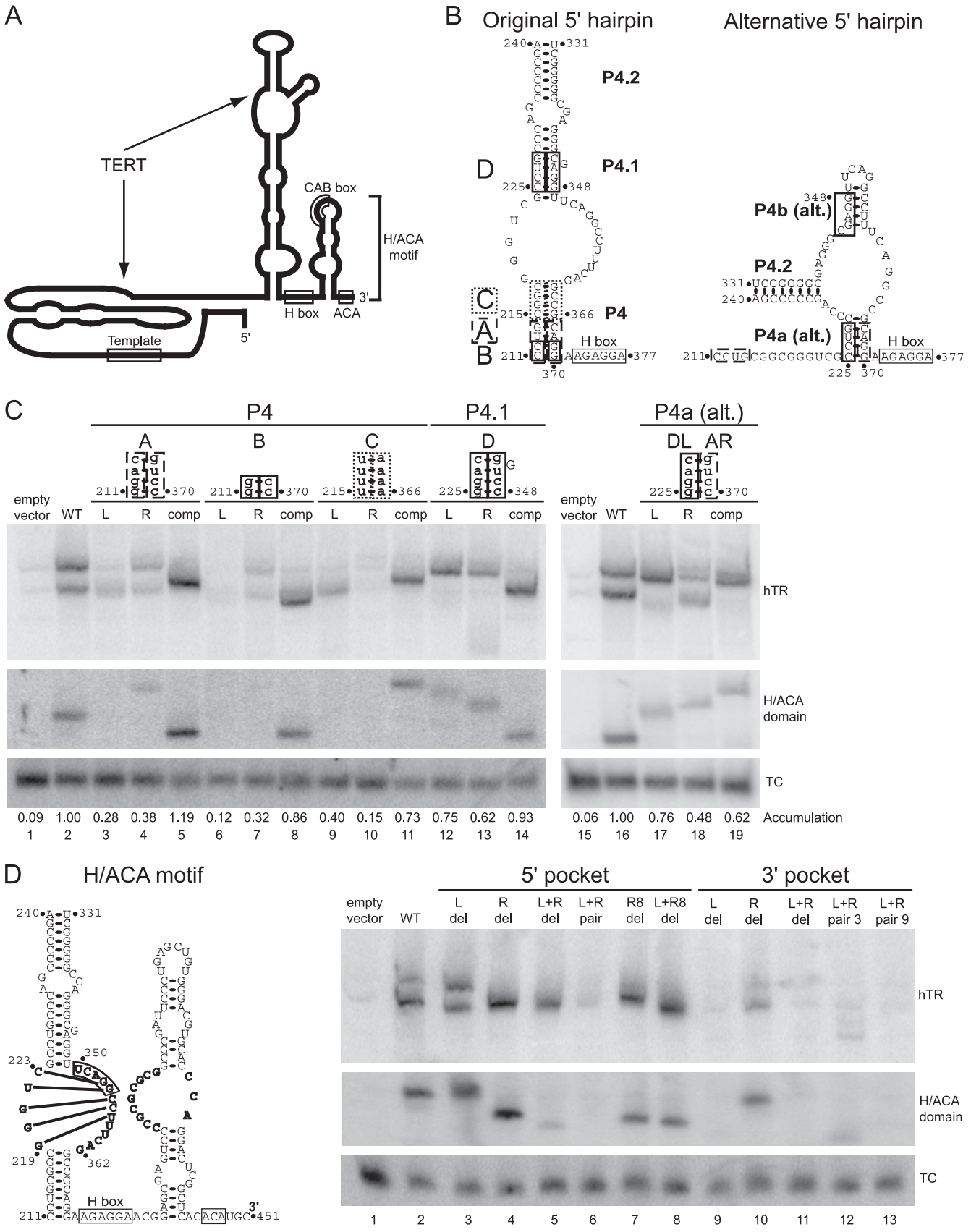

FIG. 1. The hTR H/ACA motif 5′ hairpin is noncanonical and has few structural requirements for hTR accumulation. (A) Secondary structure and primary sequence motifs of hTR are illustrated. (B) At left, the secondary structure of the originally proposed hTR H/ACA motif 5′ hairpin

tacts a large surface of RNA from the 3′ ACA through the hairpin lower stem and pocket, accounting for the conserved and catalytically essential 14- to 16-nt spacing of the ACA (or H box) and the top of the hairpin pocket (13, 25, 48). Biochemical assays and structural models of the eukaryotic H/ACA proteins suggest a conserved positioning of dyskerin and the interacting NOP10 subunit, with the other face of NOP10 binding to NHP2 to place it in the vicinity of the upper stem (32).

The human H/ACA snoRNA and scaRNA subfamilies of modification guide RNAs differ in their targets (rRNAs versus snRNAs) and in the presence of a motif in the terminal loop of their 5′ and 3′ hairpins, termed the Cajal body or CAB box (ugAG, where lowercase letters indicate reduced sequence conservation). Many RNAs, including hTR, transit nuclear Cajal bodies during biogenesis, but some, including H/ACA scaRNAs, concentrate in Cajal bodies as a steady-state distribution (26). Cajal body localization of H/ACA scaRNAs is dependent on the CAB boxes in each hairpin (33). Most vertebrate TERs have a CAB box located in the 3′ hairpin of the H/ACA motif (21, 47). Dependent on this single CAB box, hTR shows cell cycle-regulated concentration in Cajal bodies of TERT-expressing cancer cell lines (21, 22, 38, 39, 49). The hTR CAB box is not essential for telomere elongation (18), but it may increase the rate of telomere elongation or the telomere length set point when hTR is overexpressed in cancer cells (10). WDR79/TCAB1 was identified as a direct RNA binding protein dependent on a CAB box for H/ACA RNP interaction (40) and, paradoxically, as an RNA-independent interaction partner of dyskerin (42). Like the CAB box itself, WDR79/TCAB1 is not required for hTR accumulation or telomerase catalytic activity, but it is required for hTR concentration in Cajal bodies (42). Long-term depletion of WDR79/TCAB1 in a human fibrosarcoma cell line reduced telomere length (42), suggesting that hTR Cajal body concentration promotes telomere maintenance. Given that not all cells with active telomerase have Cajal bodies, WDR79/TCAB1 may more generally promote telomere maintenance by allowing hTR to escape from a default snoRNA-like sequestration in the nucleolus.

Structural similarities between hTR and other H/ACA RNAs have been established by previous studies, but differences have not been explored. Unique features of hTR H/ACA RNP assembly are likely to underlie the telomerase-specific disease phenotypes resulting from inherited human dyskerin, NOP10, and NHP2 gene mutations (2, 34). A major potential point of difference involves the unresolved structure of the hTR H/ACA motif 5′ hairpin. Previous structure/function studies of this region to investigate requirements for RNA accumulation were difficult to interpret due to mutagenesis-induced stem pairing rearrangements (29), and phylogenetic comparison did not derive a unique fold for this region due to high sequence variability among vertebrate TERs (6). The original model of the hTR H/ACA motif 5′ hairpin (28) and similar phylogenetic predictions (6, 31) all deviate from the conserved spacing of 14 to 16 nt that should separate the H box and the top of the pocket to form the contact surface for dyskerin. Therefore, unlike other human H/ACA snoRNAs and scaRNAs, hTR could assemble a set of core proteins only on the 3′ hairpin. Indeed, the hTR 3′ hairpin has been shown to support single-stem RNP assembly *in vitro* (12), and single-stem RNP assembly has been shown to occur in trypanosomes *in vivo* (41). On the other hand, mapping of an intron-expressed hTR H/ACA domain 5′ end suggested an alternative 5′ boundary for the H/ACA motif (37), which could fold a canonical 5′ hairpin with an insertion in the pocket known to occur in some snoRNAs (see below) (Fig. 1B). Because the 5′ hairpin of the H/ACA motif separates two regions of hTR critical for TERT interaction and catalytic activity (Fig. 1A), alternative configurations of 5′ hairpin stem pairing and pocket structure could influence telomerase holoenzyme activity.

Here, we define the RNA and RNP architecture of the H/ACA domain of human telomerase using holoenzyme reconstitution *in vivo*. We find support for the original model of 5′ hairpin structure and uncover an unexpected asymmetry of significance for the 5′ versus 3′ hairpin pockets that is shared by hTR and canonical snoRNAs. Curiously, most elements of hTR 5′ hairpin structure are not important for holoenzyme catalytic activity. We next elucidate the hTR interaction stoichiometry of H/ACA RNP core proteins using a tandem affinity purification strategy. Independent of all but a minimal 5′ hairpin stem and H box, two full sets of H/ACA RNP proteins assemble on each molecule of hTR. In contrast, WDR79/TCAB1 association appears as a single copy, with strong dependence on the CAB box in the hTR 3′ hairpin loop. These studies resolve open questions of telomerase subunit stoichiometry and reveal unexpected additional similarities as well as differences in the composition of telomerase, snoRNPs, and scaRNPs in human cells.

is shown with boxes around 4 or 2 nt on each side of the putative stem pairings tested by substitution. At right is shown an alternative, more canonical secondary structure model for the H/ACA motif 5′ hairpin based on a 5′ domain boundary at position 225. P4, P4.1, and P4.2 are paired elements predicted by phylogenetic comparison; P4a (alt.) and P4b (alt.) are alternative pairings of the residues involved in P4 and P4.1. (C) Total RNA from transfected 293T cells was examined by blot hybridization. Empty-vector lanes provide a background control for detection of endogenous hTR compared to recombinant wild-type (WT) hTR or the hTR variants indicated. Full-length hTR, the 5′ processed hTR H/ACA domain, and the transfection control (TC) were detected on the same blot. In the boxed and numbered regions of hTR secondary structure taken from panel B, the substituted sequences tested in panel C are specified. L and R indicate left and right side of the stem pairings as illustrated. (D) Total RNA from transfected 293T cells was examined by blot hybridization. At left is shown the hTR H/ACA motif from the most recent secondary structure model based on phylogenetic comparison. Pocket sequences are highlighted in bold. L del, R del, L+R del indicate deletion of the left, right, or combined sides of the pocket, respectively. Pairings forced in the hTR variant of lane 6 are shown with connecting lines; all other pocket residues were deleted. The five right-side pocket residues retained in the hTR variants of lanes 7 and 8 are boxed; the other eight right-side pocket residues were deleted (R8 del).

MATERIALS AND METHODS

Cell culture, constructs, and transfection. 293T cells and VA13 cells with an integrated TERT expression vector (VA13+TERT) were cultured in Dulbecco's modified Eagle's medium (DMEM) with 10% fetal bovine serum (FBS) and transiently transfected using the calcium phosphate method (29). Expression constructs for mature hTR and the hTR-U64 chimera have been previously described (16). To generate pBS-U3-hTR-U64-500 and pBS-U3-hTR H/ACA-500, mature hTR sequence in pBS-U3-hTR-500 was replaced by hTR-U64 or the H/ACA domain region of hTR (nucleotides 203 to 451), respectively. H/ACA snoRNA expression constructs pBS-U3-U64-500 and pBS-U3-ACA28-500 were similarly constructed by replacing mature hTR sequence with the mature snoRNA sequence. The functionally validated structures of the U64 5′ hairpin and the ACA28 5′ and 3′ hairpins target known modifications of human rRNA (24, 46). N-terminally tagged proteins were expressed in the backbone contexts of pcDNA-Z (where Z represents tandem protein A domains followed by a cleavage site for tobacco etch virus protease), pcDNA-F (where F represents three copies of the FLAG tag), and pcDNA-ZF. Due to extract proteolysis in the N-terminal tag region of ZF-WDR79/TCAB1, assays shown here used the extract-stable C-terminal FZ-tagged subunit. A plasmid containing *Tetrahymena thermophila* TER under the control of the human U6 Pol III promoter was used as a control for transfection efficiency (28). All constructs were verified by sequencing.

Detection of RNA and protein. RNA was purified using TRIzol according to the manufacturer's protocol (Invitrogen). Northern blot detection of hTR, hTR-U64, and the recovery control (RC) was performed using an end-labeled 2′-*O*-methyl RNA oligonucleotide complementary to hTR positions 51 to 72, as previously described (16). The 5′-processed hTR H/ACA domain alone was detected using DNA oligonucleotide probes complementary to nucleotides 305 to 335, 363 to 390, or 419 to 449, depending on the hTR variants analyzed. Endogenous and recombinant human snoRNAs were detected using DNA oligonucleotide probes complementary to positions 54 to 82 of U64 or positions 79 to 107 of ACA28. Immunoblots to detect tagged proteins used FLAG M2 monoclonal antibody or rabbit IgG primary antibody and were imaged using a Li-Cor Odyssey system.

Telomerase activity assay. Cell extracts prepared by freeze-thaw lysis (29) were clarified by centrifugation. Nine micrograms of total protein as determined by Bradford assay was used in each reaction mixture. Assay buffer contained final concentrations of 10 mM HEPES, 50 mM Tris acetate, 5% glycerol, 40 mM NaCl, 50 mM potassium acetate, 4 mM $MgCl_2$, 1 mM EGTA, 1 mM spermidine, and 5 mM β-mercaptoethanol at pH 8.0. Reactions were initiated by the addition of 500 nM telomeric repeat primer $(G_3T_2A)_3$, 0.25 mM dTTP and dATP, 5.5 μM unlabeled dGTP, and 0.33 μM [α-^{32}P]dGTP (3,000 Ci/mmol; PerkinElmer Life Sciences), and mixtures were incubated at 30°C for 1 h. The 40-μl assay volumes were supplemented with 60 μl of RNase A stop solution, incubated at 37°C for 15 min, supplemented with 50 μl of proteinase K solution, and incubated again at 37°C for 15 min. Product DNA was purified by phenol-chloroform extraction and ethanol precipitation and then analyzed by denaturing acrylamide gel electrophoresis.

Affinity purification. For tandem affinity purification of tagged dyskerin, NHP2, GAR1, TERT, and WDR79/TCAB1, cell extracts from freeze-thaw cell lysis were diluted to ~2 mg/ml in binding buffer (20 mM HEPES at pH 8.0, 150 mM NaCl, 2 mM $MgCl_2$, 0.2 mM EGTA, 10% glycerol, 0.1% Igepal, 1 mM dithiothreitol [DTT], 0.1 mM phenylmethylsulfonyl fluoride [PMSF], and 1/1,000 volume of Sigma protease inhibitor cocktail). A volume of 0.9 ml of diluted extract was clarified by centrifugation immediately prior to purification using 5 μl of packed resin. Rabbit IgG agarose (Sigma) or FLAG M2 antibody resin (Sigma) was washed three times in 1 ml of binding buffer prior to use. Samples were rotated end over end for 2 h at room temperature or overnight at 4°C. Bound samples were washed twice at room temperature in 1 ml of wash buffer [binding buffer with 0.1% Triton X-100, 0.1% CHAPS (3-[(3-cholamidopropyl)-dimethylammonio]-1-propanesulfonate), 100 ng/μl bovine serum albumin (BSA), and 100 ng/μl tRNA] for 5 min for each wash and then transferred to ultralow retention tubes (Phenix) for a third wash. To elute bound protein, a final concentration of 150 ng/μl of the 3×FLAG peptide or ~30 ng/μl of the S219V variant of tobacco etch virus protease was added in a volume of 50 μl of wash buffer, and the mixture was rotated end over end for 15 min at room temperature. Supernatant was removed, and the resin was rinsed with another 50 μl of wash buffer. The combined 100 μl of elution supernatant was cleared of contaminating beads using Micro Bio Spin columns (Bio-Rad) and added to 5 μl of the second resin. Second-step binding was performed by end-over-end rotation for 30 min at room temperature, followed by washing and elution as described above. Single-step purification of WDR79/TCAB1 was performed using Z-tagged protein under the conditions described above.

RESULTS

The hTR H/ACA motif has a noncanonical secondary structure. The first investigation of hTR H/ACA motif structure proposed a 5′ hairpin starting at position 211 (Fig. 1B, left). Consistent with studies of the *Saccharomyces cerevisiae* H/ACA snoRNAs known at that time, the hTR H box, ACA, and 3′ hairpin lower stem were each found to be essential for *in vivo* accumulation (4, 28, 29). Although the 5′ hairpin lower stem is critical for intron-encoded snoRNA accumulation, it is not essential for accumulation of an independently transcribed yeast snoRNA (4). Substitutions of the predicted hTR 5′ hairpin lower stem did not inhibit mature hTR accumulation, but changes in the size and accumulation level of the hTR H/ACA domain processed from the hTR primary transcript at its 5′ and 3′ ends suggested that mutagenesis of the 5′ hairpin created alternative stem pairings (29). A full-length hTR secondary structure prediction derived by phylogenetic comparison supported the original model of H/ACA motif structure and placed the 5′ hairpin at the base of a hypervariable stem (6). More recently, 5′ end mapping of the 5′- and 3′-end-processed hTR H/ACA domain raised the prospect of an alternative 5′ hairpin lower stem beginning at position 225 (37), which could fold a hairpin structure with canonical rather than noncanonical spacing from the H box to the top of the 5′ pocket (Fig. 1B, right). Notably, *in vivo* modification protection of hTR (1) is most consistent with the alternative secondary structure model.

To establish the pairing register of the hTR H/ACA motif 5′ hairpin, we introduced stem disruptions and stem repair combinations in the expression construct U3-TER-500, in which a Pol II snRNA promoter drives expression of hTR and its endogenous downstream flanking 500 bp. This construct produces mature hTR and catalytically active telomerase holoenzyme that is functional for telomere elongation (16, 45). Recombinant hTR was expressed by transient transfection of 293T cells, allowing a high level of recombinant RNP accumulation. Substitutions that should discriminate the original and alternative models for 5′ hairpin structure were designed in blocks of 2 to 4 nt (Fig. 1B), using folding predictions to minimize the potential for formation of alternative pairings. Every experiment included an empty vector control for endogenous hTR background. RNA was harvested from cells transfected to express recombinant versions of hTR and a ciliate TER transcribed using the human U6 snRNA Pol III promoter as a transfection control (TC). Total RNA was resolved by denaturing polyacrylamide gel electrophoresis (PAGE) and probed to detect the RNAs of interest. Due to partial folding during acrylamide gel electrophoresis, hTR typically migrates as a doublet. In this and previous studies, substitutions in the 5′ hairpin induced variability in hTR gel migration.

Single-sided substitutions of the 5′ hairpin lower stem inhibited hTR accumulation, and in each case this inhibition was rescued by the compensatory combination of left-side and right-side changes (Fig. 1C, L and R, respectively, in lanes 3 to 11). Compensatory combinations also rescued accumulation of the hTR H/ACA domain alone, albeit giving rise to migration heterogeneity that could reflect differences in size and/or par-

tial folding during electrophoresis. Notably, only two of the six single-sided stem substitutions reduced recombinant hTR accumulation to near the level of endogenous hTR background (Fig. 1C, compare lanes 1, 6, and 10) while the corresponding other-side substitutions (lanes 7 and 9) or a larger substitution involving the same residues (lane 3) was permissive for some hTR accumulation. Together, the results support the original model of a 5′ hairpin 8-bp lower stem that begins at position 211 (Fig. 1B, left) because compensatory mutagenesis rescued the loss of accumulation imposed by a 2-nt substitution at the left-side base of this stem (pairing B) or a 4-nt right-side substitution at the top of this stem (pairing C). Although the loss and rescue of accumulation are less dramatic, disruption and repair of the hTR H/ACA motif 5′ hairpin upper stem lend modest support for formation of this element as well (Fig. 1C, lanes 12 to 14).

We also investigated potential formation of the alternative 5′ hairpin stem beginning at position 225 (Fig. 1B, right). Despite its several attractions, the alternative model was not favored by mutagenesis results. The combination of putative compensatory left-side and right-side stem substitutions did not improve hTR accumulation (Fig. 1C, lanes 17 to 19). We conclude that the hTR H/ACA motif 5′ hairpin can, and likely does, begin at position 211 although alternative foldings appear to support the accumulation of mature hTR. Also, the 5′ hairpin structural requirements for full-length hTR appear more lenient than those for the hTR H/ACA domain alone, suggesting that folding of the 5′ hairpin region could differ in the full-length hTR context and in the H/ACA domain stable to 5′ processing. Overall, these findings establish differences between the architecture of the hTR H/ACA motif 5′ hairpin and the 5′ hairpins of other H/ACA RNAs.

A 5′ hairpin pocket is not required for hTR accumulation. The role of the H/ACA motif hairpin pockets in base pairing to target RNAs has been well established, but to our knowledge the significance of these pockets for canonical snoRNA accumulation and RNP assembly has not been examined. Previous studies of hTR found that both sequence substitution of the 3′ hairpin pocket and sequence tag insertion in the 5′ pocket were tolerated for accumulation while a substitution intended to force pairing of the canonically positioned 3′ pocket was not (28, 29). To directly compare the significance of the hTR 5′ and 3′ hairpin pockets, we first examined the impact of deleting the left side, right side, or left and right sides of each hairpin pocket (Fig. 1D, left; pocket residues are shown for the most recent model based on phylogenetic comparison) (31). None of the deletions within the 5′ pocket strongly reduced hTR accumulation (Fig. 1D, lanes 3 to 5). Making a smaller 5′ pocket by deleting all but five residues of the right-side pocket (boxed in Fig. 1D, left), without or with accompanying deletion of all left-side pocket residues (lane 7 or 8, respectively), also allowed hTR accumulation. In contrast, the corresponding perturbations of the 3′ pocket reduced or eliminated hTR accumulation (Fig. 1D, lanes 9 to 11).

We also tested the impact of pairing across the pocket. In the 5′ pocket, converting the pocket to a 5-bp duplex (depicted by the cross-pocket lines in the illustration of Fig. 1D) was detrimental for hTR accumulation (lane 6). We note that the long 21-bp duplex created by this pocket pairing could have indirectly led to transcript degradation. Replacement of the 3′ pocket with a 3-bp or 9-bp duplex was also detrimental for hTR accumulation (Fig. 1D, lanes 12 and 13), despite the shorter overall length of duplex that was created. In general, perturbations of pocket structure had a parallel impact on the accumulation of full-length hTR and the hTR H/ACA domain alone, although accumulation of the H/ACA domain alone was less tolerant of complete 5′ pocket deletion (Fig. 1D, lane 5). The combined results of hTR H/ACA motif pocket mutagenesis reveal additional asymmetry in the structural requirements for the 5′ and 3′ hairpins.

Holoenzyme catalytic activity is tolerant of changes in 5′ hairpin structure. The hTR H/ACA motif 5′ hairpin elements separate two TERT-interacting regions of hTR critical for catalytic activity (29). To test whether relative positioning of the two TERT-interacting regions is important for holoenzyme catalytic activity, we reconstituted hTR variants into telomerase holoenzyme by transfection of VA13 cells lacking endogenous hTR (5). VA13+TERT cells (VA13 cells with an integrated TERT expression vector) were transfected to express hTR variants that abrogate wild-type pairing of the H/ACA motif 5′ hairpin lower stem (Fig. 1B, pairing A) or upper stem (Fig. 1B, pairing D) or eliminate the 5′ hairpin pocket (Fig. 1D, L+Rdel). Telomerase activity in cell extracts was assayed by direct primer extension to monitor repeat addition processivity as well as activity overall.

Surprisingly, most H/ACA motif 5′ hairpin substitutions did not affect telomerase activity: catalytic activity generally paralleled hTR accumulation (Fig. 2). One exception was the left-side substitution of the 5′ hairpin lower stem (Fig. 2, lane 3), which could indirectly affect the folding of the adjacent template/pseudoknot region. Notably, holoenzymes with disrupted pairing of the alternative 5′ hairpin lower stem beginning at position 225 also retained catalytic activity (Fig. 2, lanes 4 and 6). We conclude that the relative positioning of TERT-interacting motifs across the intervening H/ACA motif 5′ hairpin is not important for holoenzyme catalytic activity. Sufficient TERT interaction affinity for each of its bound hTR motifs may obviate the role of other proteins in hTR-hTERT interactions.

Asymmetric 5′ and 3′ hairpin requirements are shared by canonical snoRNAs. To establish some necessity of 5′ hairpin structural elements for hTR accumulation, we sought to determine the maximal extent of the 5′ hairpin that could be deleted. We created internal truncations of the 5′ hairpin that removed the H/ACA motif upper stem (Fig. 3A, Δ1), the upper stem and pocket (Δ2), or the entire stem/pocket/stem hairpin (Δ3). Remarkably, deletions that removed the upper stem or the upper stem and pocket did not substantially affect hTR accumulation (Fig. 3A, lanes 3 and 4). A detectable level of hTR accumulated even with complete 5′ hairpin deletion (Fig. 3A, lane 5), in contrast to the undetectable accumulation of hTR variants with substitutions in the H box or ACA expressed from the same vector (data not shown).

To determine whether the minimal 5′ hairpin requirement was unique to hTR, we tested the accumulation of canonical human H/ACA snoRNAs U64 (Fig. 3B) and ACA28 (Fig. 3C) with deletions in the 5′ or 3′ hairpin. Surprisingly, for both of these snoRNAs, combined deletion of the 5′ pocket right-side and left-side residues did not reduce accumulation (Fig. 3B and C, lanes 5). Deletion of either pocket side alone had a

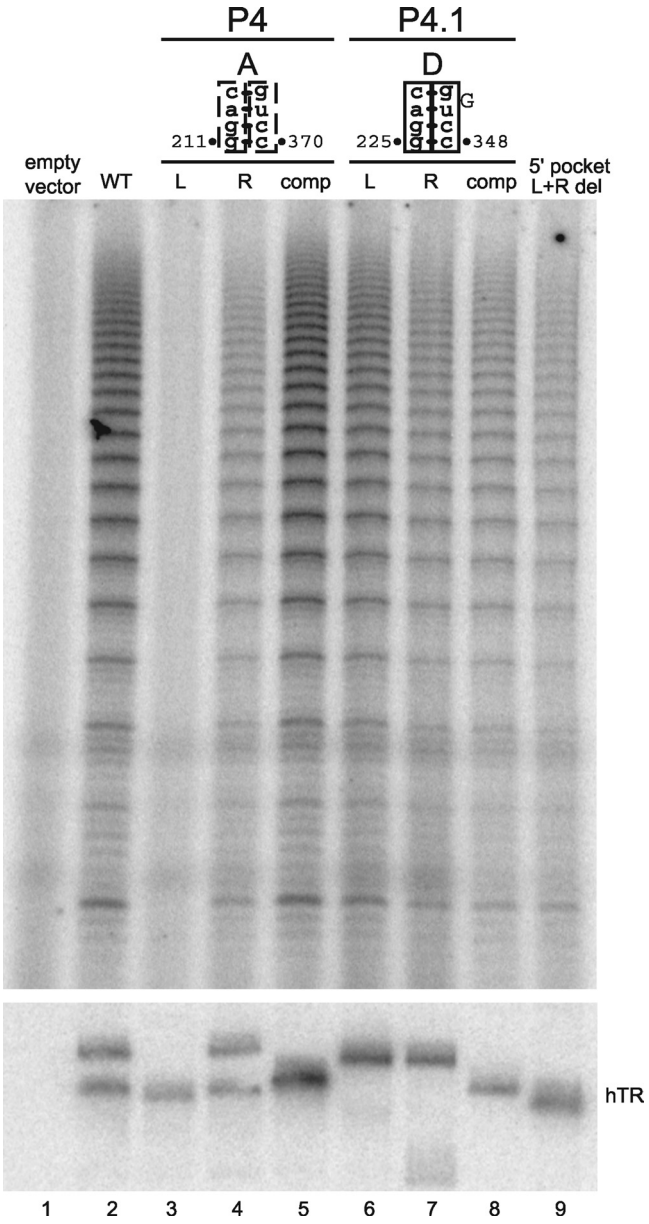

FIG. 2. Holoenzyme catalytic activity does not require any specific paired region of the 5′ hairpin stem or the 5′ hairpin pocket. Direct primer extension activity assays were performed using extracts of VA13+TERT cells transfected to express the indicated hTR variants. Levels of hTR in the extracts are shown by blot hybridization; note that the hTR variant of lane 8 was slightly underaccumulated in this set.

partially inhibitory impact, perhaps resulting from induced misfolding (Fig. 3B and C, lanes 3 and 4). Remarkably, deletions of the entire 5′ hairpin upper stem and pocket were permissive for snoRNA accumulation (Fig. 3B and C, lanes 9). In contrast to the 5′ hairpin pocket, any perturbation of the 3′ hairpin pocket was strongly inhibitory (Fig. 3B and C, lanes 6 to 8). These unexpected findings suggest that although hTR has a uniquely divergent 5′ hairpin structure, there are no fundamental differences between hTR and canonical H/ACA snoRNAs in the asymmetry of 5′ and 3′ hairpin requirements for RNP assembly *in vivo*.

The hTR H/ACA motif recruits two full sets of core proteins. Yeast H/ACA snoRNAs assemble a set of core proteins on each hairpin, as demonstrated by snoRNP gel filtration and electron microscopy (43) and cooperative function of two hairpin units *in vivo* (4). The atypically large spacing between the hTR H box and the top of the 5′ hairpin pocket and the autonomy of the hTR 3′ hairpin for H/ACA RNP assembly *in vitro* (12) suggest that the hTR 5′ hairpin may not assemble a typical set of H/ACA RNP proteins. To address whether one or both hTR H/ACA motif hairpins assemble core proteins *in vivo*, we exploited a tandem affinity purification strategy, schematized in Fig. 4A. We transiently transfected 293T cells to express plasmids encoding hTR, the hTR-U64 chimera with the 3′ half of hTR replaced by a snoRNA (29), and tagged versions of the H/ACA RNP core proteins dyskerin, NHP2, and GAR1. Tagged forms of the very small protein NOP10 accumulate poorly due to tag interference with RNP assembly (18), but because this subunit organizes the dyskerin-NOP10-NHP2 heterotrimer, its presence can be inferred from the combination of dyskerin and NHP2. Each protein was tagged with tandem protein A domains (Fig. 4, Z), a triple FLAG tag (F), or the fusion of both tags (ZF). In addition to each tagged protein expressed separately, the Z-tagged and F-tagged proteins were coexpressed (Fig. 4, +). Plasmid concentrations were optimized to yield nearly equal amounts of each tagged form of protein, as monitored by immunoblots of cell extract (data not shown).

Affinity purification was performed using panels of four transfected cell extracts in parallel (Fig. 4, Z, F, +, and ZF). First, any Z-tagged complexes were bound to IgG resin and eluted. Next, enriched Z-tagged RNPs that also harbored an F tag were bound to FLAG antibody resin and eluted. Tandem affinity-purified RNPs were supplemented with a recombinant RNA recovery control (RC) prior to RNA extraction. Purified RNA was then resolved by denaturing PAGE and interrogated by blot hybridization. For ZF-tagged protein, tandem steps of purification will recover all RNPs assembled with even a single subunit of tagged protein, but only RNP complexes containing at least two subunits of tagged protein will be recovered by tandem steps of purification from extract with the combination of Z-tagged and F-tagged protein (Fig. 4A). Purifications from extracts containing only Z-tagged or F-tagged protein serve as negative controls for nonspecific background. This methodology has demonstrated the monomeric nature of TERT and hTR in the catalytically active human telomerase holoenzyme (14).

Here, we cotransfected the hTR-U64 chimera as an internal control for tandem purification efficiency. Because U64 is a canonical snoRNA, the chimera should assemble two sets of core H/ACA proteins. Also, because hTR-U64 shares the 5′ template/pseudoknot region of hTR, the same oligonucleotide hybridization probe can be used to detect hTR and hTR-U64 simultaneously. The ratio of hTR to hTR-U64 recovered by the Z-tagged and F-tagged protein combination relative to the ZF-tagged control provides a rigorously normalized quantification of subunit stoichiometry: only if an hTR RNP harbors at least two H/ACA protein subunits will hTR be recovered from extract containing the combination of Z-tagged and F-tagged proteins, and only if the vast majority of hTR RNP assembles precisely two sets of H/ACA proteins will the ratio of hTR to

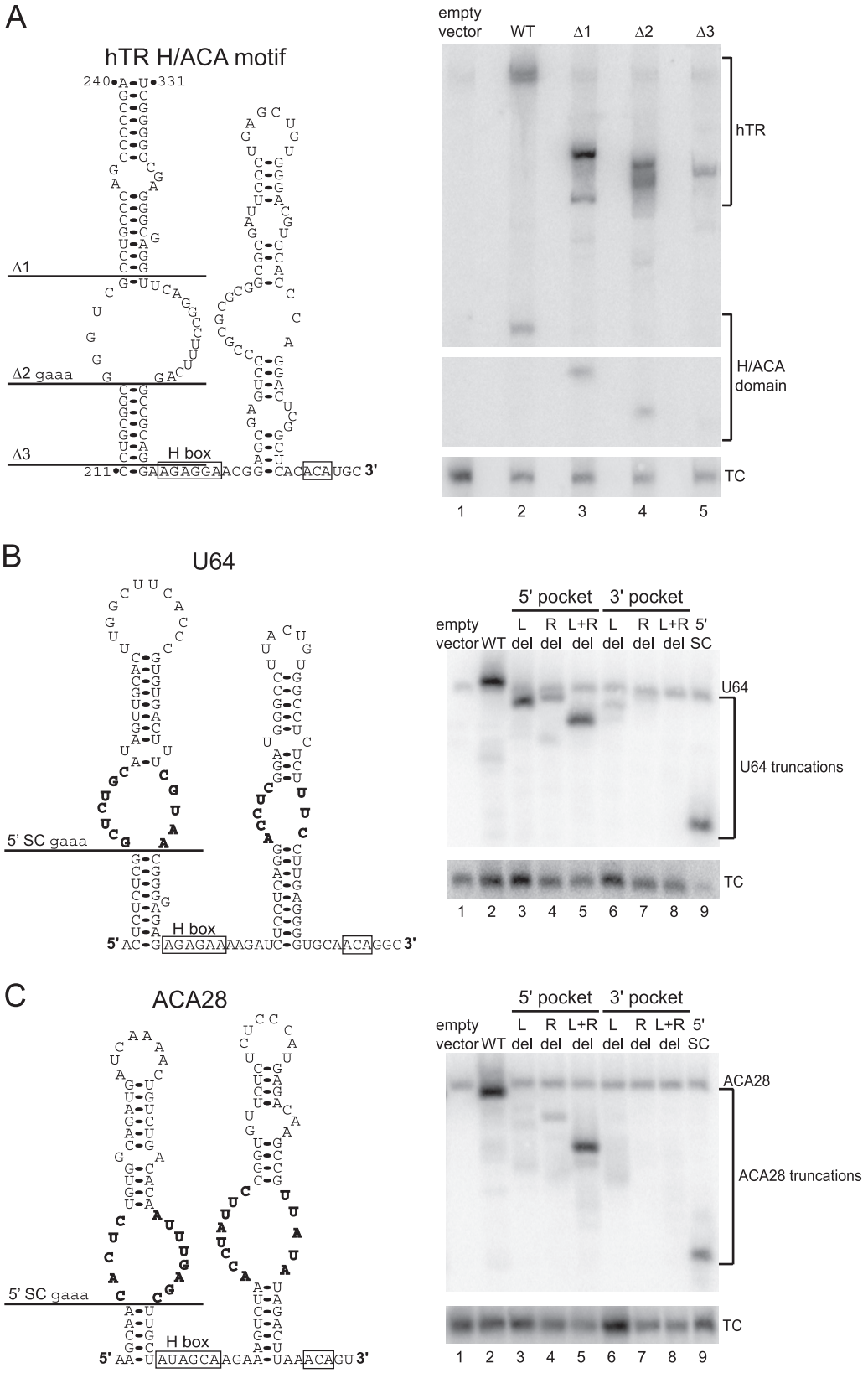

FIG. 3. A minimal 5′ hairpin stem is sufficient for accumulation of hTR and snoRNAs. Total RNA from transfected 293T cells was examined by blot hybridization. At left are shown secondary structures of the hTR H/ACA domain phylogenetic model (A), the human snoRNA U64 (B), and the human snoRNA ACA28 (C). Positions of internal deletion are indicated: Δ1, deletion of H/ACA motif upper stem; Δ2, deletion of the upper stem and pocket; Δ3, deletion of the entire stem/pocket/stem hairpin. Only hTR Δ2 and the snoRNA 5′ stem cap (SC) deletions insert a GAAA tetraloop in place of the deleted sequence. Human snoRNA pocket sequences are highlighted in bold. L del, R del, L+R del indicate deletion of the left, right, or combined left and right sides of the pocket, respectively.

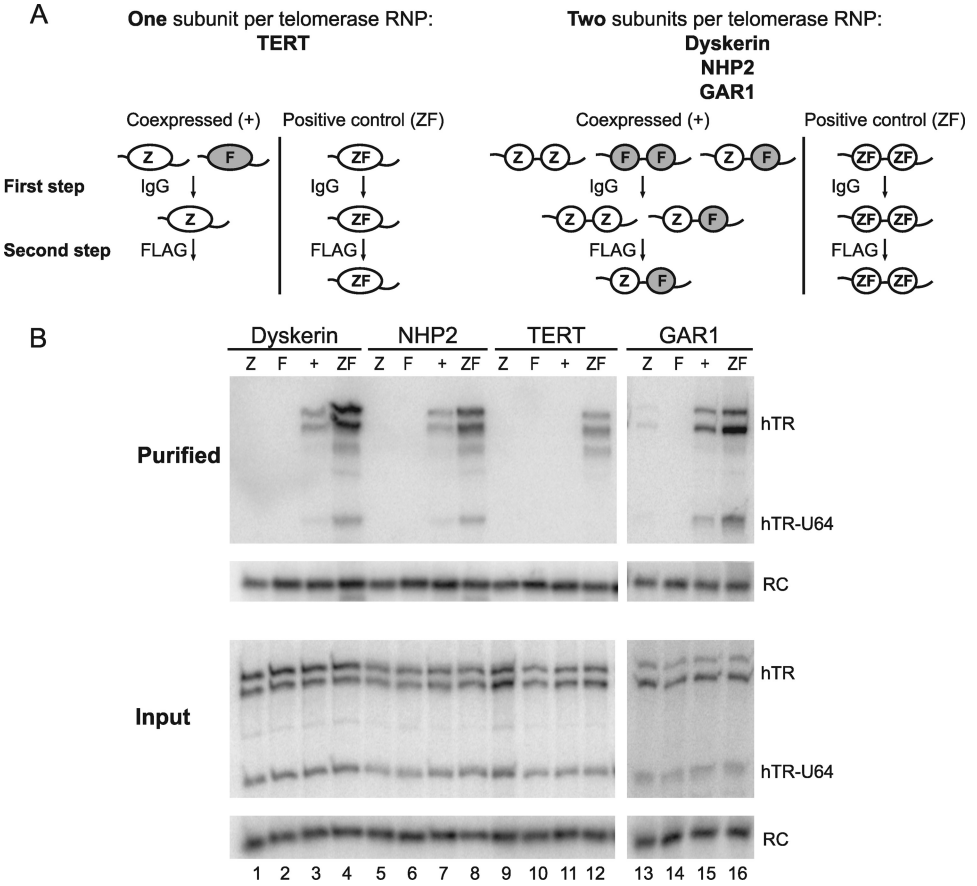

FIG. 4. Two subunits of dyskerin, NHP2, and GAR1 assemble on each molecule of hTR. (A) Schematic of the tandem affinity purification strategy for discriminating subunit stoichiometry. (B) Extracts from 293T cells transfected to express a protein with the tag(s) indicated (Z, F, +, and ZF, where + indicates coexpression of the Z and F tags), wild-type hTR, and the hTR-U64 chimera were subjected to tandem steps of affinity purification. Input cell extracts (2%) and final purified RNP elutions (100%) were supplemented with a recombinant RNA recovery control (RC) prior to RNA extraction. Input and purified samples for the GAR1 panel were from a separate set of transfections and purifications.

hTR-U64 recovered by the combination of Z-tagged and F-tagged protein versus the ZF-tagged protein be consistent.

Using tagged dyskerin and tagged NHP2 extracts (Fig. 4B, lanes 1 to 8), recovery of hTR and hTR-U64 by ZF-tagged protein was robust. Little, if any, nonspecific background was detected after tandem steps of purification from the negative-control extracts with Z-tagged or F-tagged protein alone. As expected if H/ACA RNP complexes assembled on both the 5′ and 3′ hairpins of the U64 and hTR H/ACA motif, both the hTR-U64 chimera and hTR were recovered from the extracts with coexpressed Z-tagged and F-tagged subunits. The efficiency of RNP purification by coexpressed single-tagged subunits should be less than that obtained by the double-tagged subunit, because some RNPs will assemble with two Z-tagged subunits or two F-tagged subunits instead of one of each. Notably, the ratio of hTR to hTR-U64 remained consistent in comparisons of purifications with the tagged protein combination and the ZF-tagged control (Fig. 4B, compare lane 3 to 4 and lane 7 to 8). These results indicate that H/ACA RNP proteins are deposited on both stems of the hTR H/ACA motif, despite the noncanonical nature of the hTR 5′ hairpin. This finding is consistent with the dependence of hTR accumulation on both the H box and the ACA (28). As additional controls, we confirmed that ZF-tagged TERT but not the Z-tagged and F-tagged TERT combination copurified hTR (Fig. 4B, lanes 11 and 12). TERT did not substantially enrich hTR-U64 because the chimeric RNA is missing a major motif for TERT interaction.

GAR1 differs from other core H/ACA proteins in its late assembly and its dispensability for precursor RNA processing and mature RNP stability (32). Roles proposed for GAR1 include improving the efficiency of target RNA modification and enhancing RNP nucleolar localization. Because hTR does not guide RNA modification and because only a minor percentage of hTR is stably associated with nucleoli (28), there is not an obvious functional requirement for GAR1 in the telomerase holoenzyme. GAR1 contacts dyskerin directly, but this interaction is mutually exclusive with at least one other direct dyskerin binding protein (11). GAR1 does copurify human telomerase holoenzyme, but the stoichiometry of its association could differ from that of the dyskerin-NOP10-NHP2 heterotrimer (18). Therefore, we compared GAR1 purification of hTR and hTR-U64 using the tandem affinity purification strategy. As observed for the other H/ACA RNP core proteins, the combination of Z-tagged and F-tagged GAR1 purified hTR as well as hTR-U64, and a consistent ratio of the two RNAs was

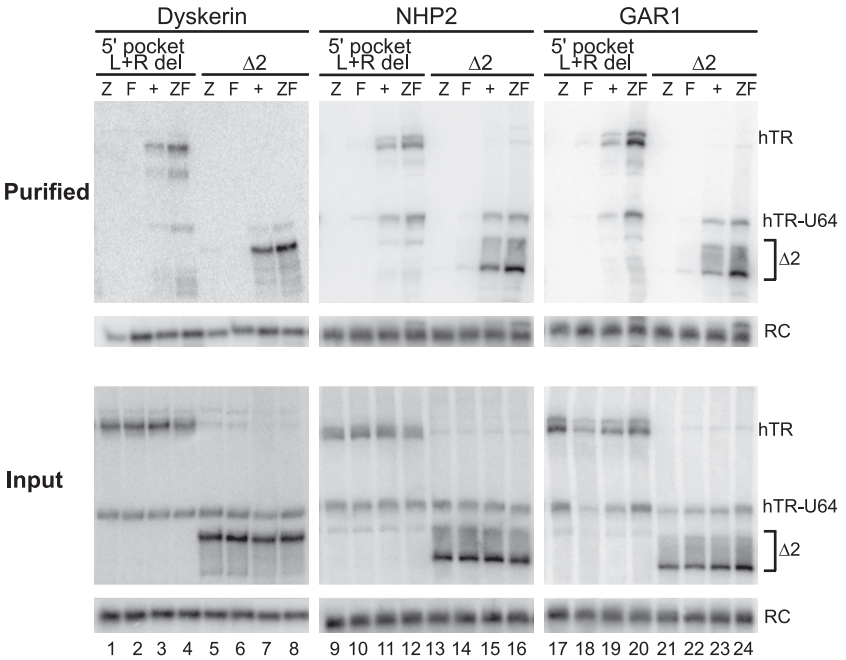

FIG. 5. Two subunits of dyskerin, NHP2, and GAR1 assemble on hTR variants lacking consensus elements of the 5′ hairpin. Extracts from 293T cells transfected to express a protein with the tag(s) indicated (Z, F, +, and ZF), hTR-U64, and one of two hTR variants (5′ pocket L+R del from Fig. 1D or Δ2 from Fig. 3A) were subjected to tandem steps of affinity purification. RNAs in the input and purified material were analyzed as described in the legend of Fig. 4. Note that hTR Δ2 migrated with different mobilities depending on sample heating. The input and purified samples of any given protein were analyzed in parallel.

obtained in purifications using the single-tag subunit combination compared to the double-tagged ZF-GAR1 (Fig. 4B, lanes 15 and 16). Importantly, analysis of RNPs from the first step of tandem purifications confirmed the expected RNP recoveries, and when the same panels of tagged dyskerin, NHP2, and GAR1 extracts were used in purifications with the order of tandem affinity purification steps reversed, parallel results were obtained (data not shown). All results were highly reproducible over independent transfections and purifications (data not shown). Together, these affinity purification assays indicate that RNP assembly on the hTR H/ACA motif yields the canonical bipartite architecture of an H/ACA snoRNP.

Assembly of two sets of H/ACA proteins requires only a minimal 5′ hairpin stem. Because most H/ACA motif elements of the hTR 5′ hairpin could be eliminated without inhibition of RNA accumulation or RNP catalytic activity, it seemed possible that one set of H/ACA proteins assembled on the 3′ hairpin would be sufficient for biogenesis of a telomerase RNP. To investigate whether removing most of the 5′ hairpin converted hTR to an archaeal-like single-stem ACA RNP, we applied the tandem affinity purification strategy to hTR variants lacking the 5′ hairpin pocket (Fig. 1D, L+R del) or lacking all nucleotides above the lower stem (Fig. 3A, Δ2; note that this RNA migrates with different mobilities depending on sample heating). These two hTR variants accumulated to sufficient levels for detection after tandem steps of affinity purification. Remarkably, both of these hTR variants assembled two subunits of dyskerin, NHP2, and GAR1 per telomerase RNP (Fig. 5, lanes 3 and 4, 7 and 8, 11 and 12, 15 and 16, 19 and 20, and 23 and 24). These findings indicate that a bipartite H/ACA RNP is assembled even when the 5′ hairpin lacks RNA elements thought to be necessary for scaffolding of protein-protein interactions. We conclude that there is a different specificity of RNP assembly on the two hairpins of the eukaryotic H/ACA motif.

WDR79/TCAB1 association with hTR has the stoichiometry and specificity of a CAB box interaction. WDR79/TCAB1 was recently discovered as a direct protein-protein interaction partner of dyskerin (42) and as a direct RNA interaction partner of the CAB box (40). We therefore wondered whether one or two subunits of WDR79/TCAB1 would assemble with hTR, given that a human telomerase RNP has two subunits of dyskerin but only one CAB box. Consistent with previous studies, hTR was detected after a single step of Z-tagged or F-tagged WDR79/TCAB1 purification on the corresponding resin (data not shown). Using the tandem affinity purification strategy described above, hTR was detected after tandem steps of purification of the double-tagged WDR79/TCAB1 (Fig. 6A, lane 8) but not after tandem steps of purification from extract with the coexpressed Z-tagged and F-tagged subunit combination (lane 7). The same result was observed regardless of the order of tandem purification steps and was reproducible for independent transfections and purifications (data not shown).

The largely single-subunit nature of WDR79/TCAB1 association with hTR predicted that its interaction would be dependent on the CAB box. Using single-step WDR79/TCAB1 affinity purification from extracts of transfected VA13+TERT cells, we compared protein association with wild-type hTR and an hTR variant with a single-nucleotide CAB box substitution sufficient to disrupt hTR concentration in Cajal bodies (21). The CAB box substitution strongly impaired but did not eliminate hTR association with WDR79/TCAB1 (Fig. 6B, lanes 5

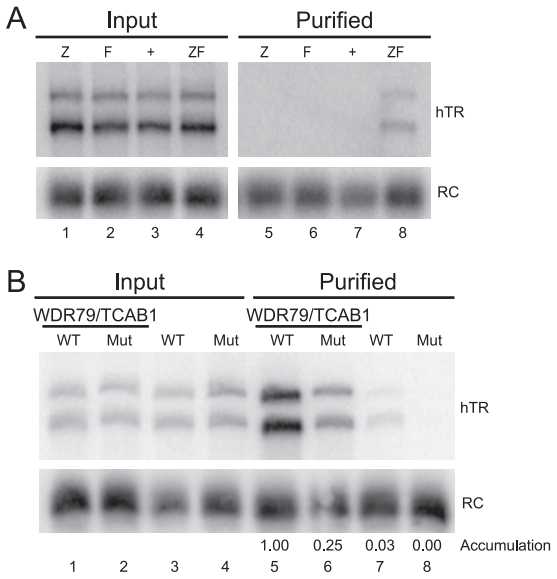

FIG. 6. Association of WDR79/TCAB1 is influenced by the hTR CAB box. (A) Extracts from 293T cells transfected to express hTR and WDR79/TCAB1 with the tag(s) indicated (Z, F, +, and ZF) were subjected to tandem steps of affinity purification. RNAs in the input and purified material were analyzed as described in the legend of Fig. 4. (B) Extracts of VA13+TERT cells transfected to express either Z-tagged WDR79/TCAB1 or empty vector and either wild-type (WT) hTR or the G414C CAB box mutant (Mut) were used for single-step affinity purification. RNAs in the input and purified material were analyzed as described above.

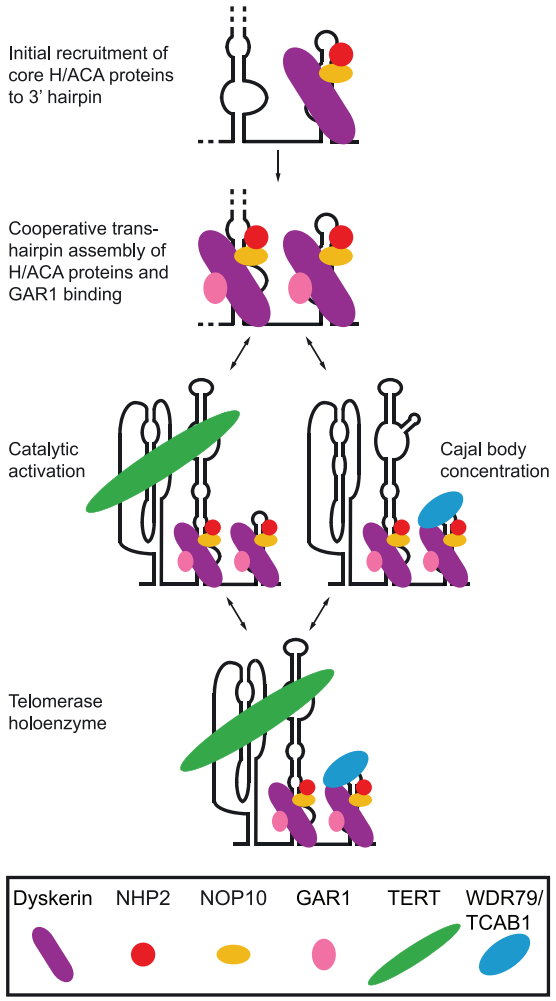

FIG. 7. Interaction specificity and stoichiometry of telomerase holoenzyme proteins. Initial recruitment of H/ACA proteins is proposed to involve an association of dyskerin, NOP10, and NHP2 with the hTR 3′ hairpin, scaffolded by extensive protein-RNA interactions. Either sequentially (as shown) or in a concerted manner, there is assembly of a second H/ACA protein heterotrimer. Assembly of the second set of H/ACA proteins is proposed to have a reduced requirement for RNA interaction surface due to the formation of cross-hairpin protein-protein interaction(s). Following hTR release from the site of transcription, an exchange of biogenesis factors for GAR1 yields the mature telomerase RNP with two full sets of all four H/ACA RNP proteins. Motifs of hTR not required for stable RNP biogenesis can associate independently with TERT and WDR79/TCAB1, both of which are likely substoichiometric in the overall population of endogenous telomerase RNP.

and 6). Similar results were obtained using extracts from transfected 293T cells (data not shown). With or without a CAB box, it seems likely that WDR79/TCAB1 binds only to the hTR 3′ hairpin loop because the loop context of the CAB box is important for Cajal body localization (37) and the hTR 5′ hairpin lacks a similarly positioned loop. Overall, our studies of human telomerase holoenzyme RNA and RNP architecture support the hTR-scaffolded steps of telomerase RNP biogenesis schematized in Fig. 7.

DISCUSSION

Unique and shared features of the hTR H/ACA motif have implications for RNP biogenesis. Elucidation of the requirements for human telomerase RNP biogenesis will bring insights for disease therapy, because differences that distinguish hTR from H/ACA snoRNAs and scaRNAs must somehow give rise to the specificity of telomerase deficiency in patients with altered dyskerin (30, 44). We first suspected that our original model for hTR 5′ hairpin folding was incorrect, based on the potential for a more canonical 5′ hairpin that satisfied the limited amount of structural data on hTR H/ACA motif folding *in vivo* (1, 37). However, extensive mutagenesis supported the original model of noncanonical 5′ hairpin secondary structure. Subsequently, the surprisingly minimal 5′ hairpin structural requirements for hTR accumulation led us to suspect that the hTR H/ACA motif was unique in its RNP assembly specificity. However, our studies of two canonical human snoRNAs revealed that they shared the hTR asymmetry of 5′ and 3′ hairpin requirements for accumulation. Another surprise was the lack of catalytic activity dependence on 5′ hairpin structure. This observation suggests that vertebrate TERT has a greater autonomy in organizing TER tertiary structure than ciliate TERT, which likewise binds two separated TER motifs but does so in a manner sensitive to the geometry of intervening stem folding by the holoenzyme protein p65 (36). Combined, these findings reveal that the noncanonical hTR H/ACA motif 5′ hairpin has evolved in a manner relatively unconstrained by requirements for mature RNA accumulation, unfettered by a requirement for function as an RNA modification

guide, and with few if any obligations to the telomeric-repeat synthesis activity of telomerase holoenzyme.

The general asymmetry of 5′ and 3′ hairpin requirements for H/ACA RNA accumulation has unexpected implications for the pathway of RNP assembly *in vivo*. Our results establish that RNP assembly on the H/ACA motif 5′ hairpin does not require the extensive protein-RNA interactions evident in structures of reconstituted archaeal single-stem RNPs (48). In contrast, RNP assembly on the H/ACA motif 3′ hairpin does appear to require this large surface of protein-RNA contact. If RNP assembly on the 5′ hairpin occurs subsequent to or in concert with RNP assembly on the 3′ hairpin, protein-protein interactions across the hairpins could allow the 5′ hairpin RNP assembly reaction to have a reduced requirement for protein-RNA interaction. Cross-hairpin interactions could be mediated by dyskerin motifs not present in the archaeal protein ortholog, a hypothesis that would account for the reduced exchange of RNP-assembled dyskerin compared to RNP-assembled NOP10 or NHP2 (23).

Holoenzyme proteins have distinct specificities and stoichiometries of hTR interaction. The RNP architecture of the human telomerase holoenzyme has been hotly debated. While several studies conclude that a complex of TERT and hTR has catalytic function only with a dimer of each subunit, others studies indicate that such dimerization is neither required nor physiological (14, 35). Also, while one study claims that the human telomerase holoenzyme contains only dyskerin, TERT, and hTR (7), other studies establish that the human telomerase holoenzyme assembles all of the core H/ACA RNP proteins (18). Most published models draw one set of H/ACA proteins per telomerase RNP, but we demonstrate that hTR assembles two full sets of H/ACA proteins. Our results define a human telomerase holoenzyme architecture in which each subunit of hTR assembles two sets of H/ACA core proteins as a prerequisite for biogenesis of a biologically stable telomerase RNP (Fig. 7). A telomerase RNP can then assemble single subunits of TERT and WDR79/TCAB1 to become the holoenzyme functional for telomere maintenance (Fig. 7). Additional hTR binding proteins actively or passively distinguish telomerase RNP subpopulations with differential localization and regulation (8).

Less hTR was recovered with tagged WDR79/TCAB1 than with any tagged H/ACA core protein after a single step of purification or after tandem purification steps using ZF-tagged protein. This lower efficiency of purification was not due to lower tagged protein expression levels because all of the tagged WDR79/TCAB1 proteins were highly overexpressed compared to any of the tagged H/ACA core proteins (data not shown). A relatively low stoichiometry of WDR79/TCAB1 association is consistent with the single peptide of WDR79/TCAB1 detected by mass spectrometry of purified holoenzyme (D. Fu and K. Collins, unpublished data) and with modification rather than protection of the CAB box in the endogenous pool of telomerase RNP (1). Because WDR79/TCAB1 was identified as a direct dyskerin binding protein (42) and because other dyskerin binding proteins that interact with the core heterotrimer trade places during RNP biogenesis and regulation (11), we hypothesized that WDR79/TCAB1 could promote telomerase function by displacing GAR1. In contrast to predictions of this model, GAR1 association with hTR was unaffected by overexpression of WDR79/TCAB1 or by hTR CAB box mutation (data not shown). Relatively low occupancy of hTR by WDR79/TCAB1 may have precluded our ability to detect binding competition with GAR1, but the CAB box dependence of WDR79/TCAB1 association with hTR suggests that it may not need to compete with GAR1 for telomerase RNP interaction. It seems plausible that the single hTR CAB box results in only partial telomerase RNP occupancy with WDR79/TCAB1 *in vivo*. The maximal single-subunit stoichiometry of WDR79/TCAB1 association with hTR distinguishes it from H/ACA snoRNAs and scaRNAs, perhaps sensitizing telomerase RNP to its unique dynamic of TERT-dependent and cell cycle-regulated partitioning between nucleoli, Cajal bodies, and nucleoplasm.

ACKNOWLEDGMENTS

This work was supported by a predoctoral fellowship from the University of California Cancer Research Coordinating Committee (E.D.E.) and NIH grant HL079585 (K.C.)

REFERENCES

1. **Antal, M., E. Boros, F. Solymosy, and T. Kiss.** 2002. Analysis of the structure of human telomerase RNA in vivo. Nucleic Acids Res. **30:**912–920.
2. **Armanios, M.** 2009. Syndromes of telomere shortening. Annu. Rev. Genomics Hum. Genet. **10:**45–61.
3. **Blackburn, E. H., and K. Collins.** 2010. Telomerase: an RNP enzyme synthesizes DNA. Cold Spring Harb. Perspect. Biol. doi:10.1101/cshperspect.a003558.
4. **Bortolin, M. L., P. Ganot, and T. Kiss.** 1999. Elements essential for accumulation and function of small nucleolar RNAs directing site-specific pseudoruidylation of ribosomal RNAs. EMBO J. **18:**457–469.
5. **Bryan, T., L. Marusic, S. Bacchetti, M. Namba, and R. R. Reddel.** 1997. The telomere lengthening mechanism in telomerase-negative immortal human cells does not involve the telomerase RNA subunit. Hum. Mol. Genet. **6:**921–926.
6. **Chen, J. L., M. A. Blasco, and C. W. Greider.** 2000. Secondary structure of vertebrate telomerase RNA. Cell **100:**503–514.
7. **Cohen, S. B., M. E. Graham, G. O. Lovrecz, N. Bache, P. J. Robinson, and R. R. Reddel.** 2007. Protein composition of catalytically active human telomerase from immortal cells. Science **315:**1850–1853.
8. **Collins, K.** 2008. Physiological assembly and activity of human telomerase complexes. Mech. Ageing Dev. **129:**91–98.
9. **Collins, K.** 2009. Forms and functions of telomerase RNA, p. 285–301. *In* N. G. Walter, S. A. Woodson, and R. T. Batey (ed.), Non-protein coding RNAs. Springer-Verlag, Berlin, Germany.
10. **Cristofari, G., E. Adolf, P. Reichenbach, K. Sikora, R. M. Terns, M. P. Terns, and J. Lingner.** 2007. Human telomerase RNA accumulation in Cajal bodies facilitates telomerase recruitment to telomeres and telomere elongation. Mol. Cell **27:**882–889.
11. **Darzacq, X., N. Kittur, S. Roy, Y. Shav-Tal, R. H. Singer, and U. T. Meier.** 2006. Stepwise RNP assembly at the site of H/ACA RNA transcription in human cells. J. Cell Biol. **173:**207–218.
12. **Dragon, F., V. Pogacic, and W. Filipowicz.** 2000. In vitro assembly of human H/ACA small nucleolar RNPs reveals unique features of U17 and telomerase RNAs. Mol. Cell. Biol. **20:**3037–3048.
13. **Duan, J., L. Li, J. Lu, W. Wang, and K. Ye.** 2009. Structural mechanism of substrate RNA recruitment in H/ACA RNA-guided pseudouridine synthase. Mol. Cell **34:**427–439.
14. **Errington, T. M., D. Fu, J. M. Wong, and K. Collins.** 2008. Disease-associated human telomerase RNA variants show loss of function for telomere synthesis without dominant-negative interference. Mol. Cell. Biol. **28:**6510–6520.
15. **Feng, J., W. D. Funk, S. Wang, S. L. Weinrich, A. A. Avilion, C. Chiu, R. R. Adams, E. Chang, R. C. Allsopp, J. Yu, S. Le, M. West, C. B. Harley, W. H. Andrews, C. W. Greider, and B. Villeponteau.** 1995. The RNA component of human telomerase. Science **269:**1236–1241.
16. **Fu, D., and K. Collins.** 2003. Distinct biogenesis pathways for human telomerase RNA and H/ACA small nucleolar RNAs. Mol. Cell **11:**1361–1372.
17. **Fu, D., and K. Collins.** 2006. Human telomerase and Cajal body ribonucleoproteins share a unique specificity of Sm protein association. Genes Dev. **20:**531–536.
18. **Fu, D., and K. Collins.** 2007. Purification of human telomerase complexes identifies factors involved in telomerase biogenesis and telomere length regulation. Mol. Cell **28:**773–785.
19. **Gilson, E., and V. Geli.** 2007. How telomeres are replicated. Nat. Rev. Mol. Cell Biol. **8:**825–838.

20. **Henras, A. K., C. Dez, and Y. Henry.** 2004. RNA structure and function in C/D and H/ACA s(no)RNPs. Curr. Opin. Struct. Biol. **14:**335–343.
21. **Jády, B. E., E. Bertrand, and T. Kiss.** 2004. Human telomerase RNA and box H/ACA scaRNAs share a common Cajal body-specific localization signal. J. Cell Biol. **164:**647–652.
22. **Jády, B. E., P. Richard, E. Bertrand, and T. Kiss.** 2006. Cell cycle-dependent recruitment of telomerase RNA and Cajal bodies to human telomeres. Mol. Biol. Cell **17:**944–954.
23. **Kittur, N., X. Darzacq, S. Roy, R. H. Singer, and U. T. Meier.** 2006. Dynamic association and localization of human H/ACA RNP proteins. RNA **12:**2057–2062.
24. **Lestrade, L., and M. J. Weber.** 2006. snoRNA-LBME-db, a comprehensive database of human H/ACA and C/D box snoRNAs. Nucleic Acids Res. **34:**D158–162.
25. **Liang, B., J. Zhou, E. Kahen, R. M. Terns, M. P. Terns, and H. Li.** 2009. Structure of a functional ribonucleoprotein pseudouridine synthase bound to a substrate RNA. Nat. Struct. Mol. Biol. **16:**740–746.
26. **Matera, A. G., and K. B. Shpargel.** 2006. Pumping RNA: nuclear bodybuilding along the RNP pipeline. Curr. Opin. Cell Biol. **18:**317–324.
27. **Matera, A. G., R. M. Terns, and M. P. Terns.** 2007. Non-coding RNAs: lessons from the small nuclear and small nucleolar RNAs. Nat. Rev. Mol. Cell Biol. **8:**209–220.
28. **Mitchell, J. R., J. Cheng, and K. Collins.** 1999. A box H/ACA small nucleolar RNA-like domain at the human telomerase RNA 3′ end. Mol. Cell. Biol. **19:**567–576.
29. **Mitchell, J. R., and K. Collins.** 2000. Human telomerase activation requires two independent interactions between telomerase RNA and telomerase reverse transcriptase in vivo and in vitro. Mol. Cell **6:**361–371.
30. **Mitchell, J. R., E. Wood, and K. Collins.** 1999. A telomerase component is defective in the human disease dyskeratosis congenita. Nature **402:**551–555.
31. **Podlevsky, J. D., C. J. Bley, R. V. Omana, X. Qi, and J. J. Chen.** 2008. The telomerase database. Nucleic Acids Res. **36:**D339–343.
32. **Reichow, S. L., T. Hamma, A. R. Ferre-D'Amare, and G. Varani.** 2007. The structure and function of small nucleolar ribonucleoproteins. Nucleic Acids Res. **35:**1452–1464.
33. **Richard, P., X. Darzacq, E. Bertrand, B. E. J.ády, C. Verheggen, and T. Kiss.** 2003. A common sequence motif determines the Cajal body-specific localization of box H/ACA scaRNAs. EMBO J. **22:**4283–4293.
34. **Savage, S. A., and B. P. Alter.** 2008. The role of telomere biology in bone marrow failure and other disorders. Mech. Ageing Dev. **129:**35–47.
35. **Sekaran, V. G., J. Soares, and M. B. Jarstfer.** 2010. Structures of telomerase subunits provide functional insights. Biochim. Biophys. Acta **1804:**1190–1201.
36. **Stone, M. S., M. Mihalusova, C. M. O'Connor, R. Prathapam, K. Collins, and X. Zhuang.** 2007. Stepwise protein-mediated RNA folding directs assembly of telomerase ribonucleoprotein. Nature **446:**458–461.
37. **Theimer, C. A., B. E. J.ády, N. Chim, P. Richard, K. E. Breece, T. Kiss, and J. Feigon.** 2007. Structural and functional characterization of human telomerase RNA processing and Cajal body localization signals. Mol. Cell **27:**869–881.
38. **Tomlinson, R. L., E. B. Abreu, T. Ziegler, H. Ly, C. M. Counter, R. M. Terns, and M. P. Terns.** 2008. Telomerase reverse transcriptase is required for the localization of telomerase RNA to Cajal bodies and telomeres in human cancer cells. Mol. Biol. Cell **19:**3793–3800.
39. **Tomlinson, R. L., T. D. Ziegler, T. Supakorndej, R. M. Terns, and M. P. Terns.** 2006. Cell cycle-regulated trafficking of human telomerase to telomeres. Mol. Biol. Cell **17:**955–965.
40. **Tycowski, K. T., M. D. Shu, A. Kukoyi, and J. A. Steitz.** 2009. A conserved WD40 protein binds the Cajal body localization signal of scaRNP particles. Mol. Cell **34:**47–57.
41. **Uliel, S., X. H. Liang, R. Unger, and S. Michaeli.** 2004. Small nucleolar RNAs that guide modification in trypanosomatids: repertoire, targets, genome organisation, and unique functions. Int. J. Parasitol. **34:**445–454.
42. **Venteicher, A. S., E. B. Abreu, Z. Meng, K. E. McCann, R. M. Terns, T. D. Veenstra, M. P. Terns, and S. E. Artandi.** 2009. A human telomerase holoenzyme protein required for Cajal body localization and telomere synthesis. Science **323:**644–648.
43. **Watkins, N. J., A. Gottschalk, G. Neubauer, B. Kastner, P. Fabrizio, M. Mann, and R. Lührmann.** 1998. Cbf5p, a potential pseudouridine synthase, and Nhp2p, a putative RNA-binding protein, are present together with Gar1p in all H BOX/ACA-motif snoRNPs and constitute a common bipartite structure. RNA **4:**1549–1568.
44. **Wong, J. M., M. J. Kyasa, L. Hutchins, and K. Collins.** 2004. Telomerase RNA deficiency in peripheral blood mononuclear cells in X-linked dyskeratosis congenita. Hum. Genet. **115:**448–455.
45. **Wong, J. M. Y., and K. Collins.** 2006. Telomerase RNA level limits telomere maintenance in X-linked dyskeratosis congenita. Genes Dev. **20:**2848–2858.
46. **Xiao, M., C. Yang, P. Schattner, and Y. T. Yu.** 2009. Functionality and substrate specificity of human box H/ACA guide RNAs. RNA **15:**176–186.
47. **Xie, M., A. Mosig, X. Qi, Y. Li, P. F. Stadler, and J. J. Chen.** 2008. Structure and function of the smallest vertebrate telomerase RNA from teleost fish. J. Biol. Chem. **283:**2049–2059.
48. **Ye, K.** 2007. H/ACA guide RNAs, proteins and complexes. Curr. Opin. Struct. Biol. **17:**287–292.
49. **Zhu, Y., R. L. Tomlinson, A. A. Lukowiak, R. M. Terns, and M. P. Terns.** 2004. Telomerase RNA accumulates in Cajal bodies in human cancer cells. Mol. Biol. Cell **15:**81–90.